

Research article

## Heavy Metal Exposure Alters Immunological Pathways Involved in Asthma Pathogenesis

Sierra L. Single<sup>1</sup>, Kenneth P Hough<sup>1</sup>, Sruti Sivan<sup>1</sup>, Mohammad Athar<sup>2</sup>, Kayla F. Goliwas<sup>\*1</sup>, and Jessy S. Deshane<sup>\*1,5</sup>

1.Division of Pulmonary, Allergy, and Critical Care Medicine, Department of Medicine, University of Alabama at Birmingham, Birmingham AL, 35294

2.Department of Dermatology, University of Alabama at Birmingham, Birmingham AL, 35294

**\*Corresponding author:** Kayla F. Goliwas ,Instructor. Department of Medicine, Division of Pulmonary Allergy and Critical Care Medicine, THH 458, 1900 University Boulevard, University of Alabama at Birmingham ,AL 35294-0006 (205) 996-2037

Jessy Deshane, Ph.D. Professor. Department of Medicine, Division of Pulmonary Allergy and Critical Care Medicine, THH 433A, 1900 University Boulevard, University of Alabama at Birmingham, 35294 Tel: 1-205-996-2041

Received: February 03, 2025; Accepted: February 27, 2025; Published: March 04, 2025

### Abstract

Heavy metal (HM) exposure is known to cause inflammation and oxidative stress, leading to respiratory diseases like asthma. However, the underlying signaling pathways that are induced during HM exposures of the lung are still being investigated. We reported earlier that HM exposure differentially modulates oxidative stress pathways, including interferon signaling and enzymatic regulation of sphingolipid metabolism, which may contribute to airway remodeling. Here, we utilized a model of HM exposure in a 3D human lung perfusion bioreactor system combined with spatial transcriptomic approaches to investigate further whether HM-induced oxidative stress resulted in activation of damaged DNA sensing pathways, mitochondrial stress, and complement cascade, and contributed to the enhanced gene alterations related to inflammation and airway remodeling often associated with asthma. We report that NaAsO<sub>2</sub> exposure had the broadest impact in gene expression alterations of sphingolipid metabolism, complement cascade, DNA sensing (STING), mitophagy, inflammasome, and airway remodeling pathways, compared to cadmium and manganese. Cell deconvolution and correlation analyses were performed to determine how abundance of lung cell populations correlated with gene expression changes following HM exposure. Changes in the complement cascade genes from NaAsO<sub>2</sub> exposure correlated with the abundance of both innate and adaptive immune cells that are implicated in asthma, confirming the role of complement as a modulator of innate and adaptive responses. Positive correlation was observed between the NaAsO<sub>2</sub>-induced innate immune signaling pathways including STING, mitophagy and inflammasome, as well as airway remodeling genes. Our studies indicate that HM-mediated oxidative stress and downstream induction of complement cascade and inflammatory signaling may contribute to asthma pathogenesis.

### Introduction

Particulate matter (PM), formed by atmospheric reactions to pollutants, varies in size and can remain suspended in the air for extended periods [1,2]. Particles smaller than ten micrometers in diameter, commonly associated with respiratory diseases, present significant health risks due to their ability to penetrate deep into the lungs, and in some cases, enter the bloodstream [2]. PM is known to reduce air quality, leading to increased respiratory morbidity and multiple clinical symptoms [3]. Notably, certain PMs contain heavy metals (HM), such as cadmium, chromium, nickel, and arsenic [4]. Inhalation of HM-bound PMs can result in their accumulation in lung tissues that may trigger cell and tissue death/injury-induced inflammatory signaling and oxida-

tive stress, often associated with chronic lung diseases [5,6]. PM exposure has been linked to the development of chronic obstructive pulmonary disease (COPD) in non-smokers, highlighting the role of environmental pollutants in pathogenesis of respiratory disease independent of smoking-related risk factors [7]. PM exposure also modulates lipid metabolism, which contributes to injury and inflammation in asthma [8].

Lungs have a large surface area, abundant oxygen, and high blood supply, making them susceptible to oxidative stress and reactive oxygen species (ROS)-mediated lung disorders, such as asthma. Asthma is characterized by increased IgE levels, eosinophilic inflammation, airway hyperresponsiveness (AHR), and reversible expiratory airflow obstruction [9]. This disease is

driven primarily by Th2 immune responses and innate lymphoid cells, which release pro-inflammatory cytokines that trigger eosinophilic inflammation. Eosinophils release reactive free radicals—such as superoxide anion, hydrogen peroxide, and hydroxyl radicals—via oxidative enzymes, creating an oxidative lung microenvironment that damages airway cells, induces inflammatory signaling, and exacerbates asthma symptoms [10].

Oxidative stress due to HM exposure is known to increase DNA damage [11] and trigger the release of double-stranded DNA (dsDNA), which can be “sensed” by cytosolic DNA-sensing cyclic GMP-AMP Synthase (cGAS) and downstream Stimulator of Interferon Genes (STING) to induce inflammation [12–19]. The cytosolic-DNA–STING axis has also been linked with inflammation and oxidative stress in murine LPS-induced lung injury models [20]. Allergen-induced oxidative stress can also cause DNA damage [21–25]. STING recruits and activates protein complexes that regulate inflammatory interferon signaling [15,26].

In lung disorders, mitochondrial ROS-mediated signaling also plays a critical role. Administration of a mitochondrial ROS inhibitor improved features of asthma in murine models of asthma with *Aspergillus fumigatus* [27]. PM exposure-induced oxidative stress has been reported to cause mitochondrial fission by enhancing fission-promoting proteins and suppressing fusion-promoting proteins in vivo in mice [27]. In rat lungs, PM exposure alters the mitochondrial structure, induces mitochondrial swelling, and increases expression of mitochondrial fission/fusion [28]. Mitophagy, a process by which damaged mitochondria are shuttled out from injured cells or tissue, can be triggered by PM exposure, contributing to the development of asthma. Environmental pollutants like acrolein were shown to induce mitophagy-related PINK1 stabilization and translocation to mitochondria, followed by mitochondrial fission [29], thus altering the mitophagy cycle and inducing pathogenic changes in airway cells in asthma.

The nucleotide-binding oligomerization domain-like receptor pyrin domain-containing protein 3 (NLRP3) inflammasome plays an important role in PM-exposure-induced asthma. This multi-protein holoenzyme is composed of the sensor protein NLRP3, two adapter proteins, and a cysteine protease [30]. When PM stimulates cells, NLRP3 can recruit the adapter protein and protease to form the NLRP3 inflammasome assembly. PM-mediated inflammasome activation involves frustrated phagocytosis, plasma membrane perturbation and potassium (K<sup>+</sup>) efflux, oxidative stress, lysosomal damage, and cathepsin B release [31]. Although the precise mechanisms remain unclear, the inflammasome has been implicated in asthma pathogenesis [32].

Recent studies have implicated complement cascade activation in asthma exacerbations. The complement cascade is a component of the innate immune response that defends against invading pathogens through the classical, lectin, or alternative pathway. PM exposure on human umbilical cord endothelial cells increased the production of ROS and activated the complement system via the alternative pathway [33]. C3a is a product of the complement system, and its production at airway surfaces can induce Th2-mediated inflammatory responses to PM-induced asthma [34]. C3a is involved in eosinophil and mast cell activation, smooth muscle contraction, and regulation of vascular

permeability [35]. A high concentration of C3a is associated with asthma hospitalization and exacerbation of allergic asthma [36]. Collectively, mitochondrial signaling, inflammasome activation, and complement pathway stimulation all release ROS that can intensify asthma symptoms upon PM exposure.

Our hypothesis is that PM exposure in the human lung modulates sphingolipid metabolism, potentially exacerbating asthma. Using human lung tissue that has been exposed to cadmium chloride, sodium arsenite, or manganese chloride, we employed GeoMX Digital Spatial Profiling to determine how gene expression changes in sphingolipid metabolism, complement, inflammasome, and mitochondrial signaling pathways were altered in response to HM exposure.

## Methods - Human Lung (3D)-Perfusion Bioreactor

De-identified, remnant human uninvolved lung specimens were obtained from lobectomy and wedge resection surgeries performed at the University of Alabama at Birmingham through collaboration with the UAB Tissue Biorepository. Uninvolved remnant human lung tissue cores were cultured ex vivo using a three-dimensional (3D) perfusion bioreactor as described in [67,68]. Briefly, six 3 mm tissue cores were placed within an extracellular matrix (ECM) support (90% collagen type I) (Advanced Biomatrix, Carlsbad, CA, USA) + 10% growth factor-reduced Matrigel (Corning, Tewksbury, MA, USA) in the central chamber of a perfusion bioreactor. Following ECM polymerization and through-channel generation, bioreactors were continuously perfused with a defined (serum-free) tissue culture media (50/50 mixture of Bronchial Epithelial Cell Growth Media) (Lonza, Walkersville, MD, USA) and X-Vivo-15 (Lonza). Following an establishment period of three days, tissues were exposed to 20 μM NaAsO<sub>2</sub>, 120 μM of CdCl<sub>2</sub>, or 100 μM of MnCl<sub>2</sub> for 8 days. Following exposure, tissue cores were fixed for histologic (formalin-fixed paraffin-embedded) analysis. This study was approved by the University of Alabama at Birmingham Institutional Review Board (IRB-#300003092) and conducted following approved guidelines and regulations.

## Tissue Microarray Generation

A tissue microarray was generated by UAB Pathology Core Research Laboratory using formalin-fixed paraffin-embedded samples with duplicate 2 mm diameter tissue cores utilized for each patient sample. Four tissues exposed to MnCl<sub>2</sub> (8 tissue cores), 2 tissues exposed to NaAsO<sub>2</sub> (4 tissue cores), 3 tissues exposed to CdCl<sub>2</sub> (6 tissue cores), and matched controls (16 tissue cores) were included. Freshly cut 5-micron TMA sections were utilized for GeoMx Digital Spatial Profiling.

## GeoMx Digital Spatial Profiling

Spatial transcriptomic profiling was completed on the TMA described above using the GeoMx Digital Spatial Profiler (DSP) (DSP-01-01, VHDX Version 3.1.0.6) with the GeoMx Human Whole Transcriptome Atlas (NanoString Technologies, Seattle, WA, USA). Briefly, a FFPE TMA section was incubated overnight at 38 °C followed by an additional 2 h at 60 °C. The section was then manually stained with the Human Whole Transcriptome Atlas UV-cleavable barcoded RNA probes along with antibodies against human Pancytokeratin and CD45, as well as SYTO 13 for geometric region of interest (ROI) selection. Using the

GeoMx DSP, ROIs were selected, and barcoded RNA probes were cleaved and collected from each ROI. Library Prep with Seq Code primers was performed and the library was sequenced on an Illumina NovaSeq 6000 sequencing instrument. FASTQ files were then converted into digital count conversion (DCC) files using GeoMx NGS Pipeline and uploaded onto the GeoMx Analysis Platform. Data then underwent quality control and Q3 normalization prior to analysis. Clustered heatmaps were generated and unpaired Student's t-tests with Benjamini–Hochberg correction were performed to compare HM to vehicle control. Clustered heatmaps were generated to display the significantly upregulated and downregulated genes with the different metal treatments. Volcano plots were generated to show the measure of significance ( $-\log_{10}$  of p-values) vs. the difference in geometric means of probe expression between HM and vehicle control. Additionally, volcano plots comparing the difference in gene expression changes with the different metal treatments and volcano plots highlight gene expression in relation to sphingolipid signaling pathways. Cell deconvolution comparing the different heavy metal treatments with controls was performed. Using this data, abundance scores and proportion of fitted cells were performed with each metal treatment. Additionally, untargeted Gene Ontology analysis and targeted Gene Set Enrichment analysis were completed in R (version 4.3.2).

### Statistical Analysis

Statistical analyses were performed using the GeoMx Analysis Platform or R. Non-paired student's T-test with Benjamini–Hochberg correction and cluster analyses were performed using GeoMx Analysis platform. A p-value less than 0.05 was considered to be statistically significant. All analyses were performed using R version 4.3.2 ("Eye Holes") on a 64-bit Linux platform (x86\_64-pc-linux-gnu). Data processing and statistical analysis were conducted using custom R scripts with several packages from the Bioconductor and CRAN ecosystems. Raw gene expression data were preprocessed to extract and format metadata (e.g., treatment, sample ID), remove headers, and transpose data matrices to a sample-wise format. Expression values were merged with metadata, and gene expression columns were coerced to numeric types for downstream analysis. Curated gene sets representing biologically relevant pathways, such as STING-mediated immune response, airway remodeling, sphingolipid metabolism, complement activation, inflammasome, mitophagy, and lymphocyte activation, were defined manually based on known functional roles defined by NanoString. To assess pathway interactions, pairwise Pearson correlations were computed between gene expression differences (treatment vs. control) across all pathway gene pairs. Significance was assessed using correlation p-values, which were adjusted for multiple testing using the Benjamini–Hochberg (BH) method. Results were visualized as dot plots using the ggplot2 package, with dot size representing  $-\log_{10}(p)$  and color reflecting correlation strength. Cell-type-specific analyses were performed by correlating gene expression ( $\log_2$  fold-changes) with cell-type proportion estimates derived from deconvolution data. Correlation statistics were computed using `cor.test()`, and summarized visually using dynamic dot plots. Gene Set Enrichment Analysis (GSEA) was performed using the clusterProfiler package

(v4.10.0), along with DOSE, enrichplot, and GOpilot, utilizing Gene Ontology (GO) annotations from the org.Hs.eg.db (human genome annotation) package. Genes were ranked by  $\log_2$  fold-change, and GSEA was conducted separately for Biological Process (BP), Molecular Function (MF), Cellular Component (CC), and the union of all ontologies. Significant enrichments (adjusted  $p < 0.05$ ) were visualized using split dot plots. For pathway-level summaries, one-way ANOVA was performed per gene across treatment groups to identify the top 20 differentially expressed genes within each pathway. For each treatment group, two-sample t-tests were used to compare treated and control conditions, and gene-level summary statistics, including means,  $\log_2$  fold-change, and adjusted p-values, were compiled. Results were visualized as  $\log_2$  fold-change heatmaps using the ComplexHeatmap package, clustered by gene where appropriate.

### Results

Dysregulation of sphingolipid metabolism has been increasingly implicated in the pathogenesis of chronic lung diseases such as asthma, due to its role in regulating inflammation, cell survival, and barrier integrity in lung tissues [37]. Heavy metals (HMs) like arsenic ( $\text{NaAsO}_2$ ), cadmium ( $\text{CdCl}_2$ ), and manganese ( $\text{MnCl}_2$ ) are environmental pollutants known to induce oxidative stress and inflammatory responses, potentially exacerbating lung disease processes. Previous studies, including our own, have shown that HM exposure alters gene expression related to oxidative stress and immune signaling pathways in bronchial epithelial cells and lung tissues [38].

Given this background, we sought to investigate the specific transcriptional effects of HMs on genes involved in sphingolipid metabolism, which is critical for maintaining cellular homeostasis and immune regulation in the lung. The use of clustered heatmaps and volcano plots allows for the visualization and identification of significant gene expression changes upon exposure to different HMs, providing a comprehensive view of the molecular perturbations.

The differential gene expression profiles observed, particularly the stronger upregulation of sphingolipid metabolism genes in  $\text{NaAsO}_2$ -treated tissues compared to  $\text{CdCl}_2$  and  $\text{MnCl}_2$ , suggest that arsenic exposure may uniquely influence the sphingolipid rheostat, potentially through more pronounced oxidative or inflammatory signaling. The overlapping gene alterations (e.g., *SPNS2*, *DEGS2*, *UGT8*, *ARSI*) further highlight shared molecular targets of these metals, while unique patterns (e.g., *ARSH*, *GLB1L*, *CERS3*, *CERS4*) indicate metal-specific effects on sphingolipid pathway components.

To understand the biological relevance of these transcriptional changes, it is crucial to relate them to specific cell populations within the lung, as different cell types contribute distinctly to lung function and immune responses. Cell deconvolution analyses, which computationally infer the proportions of immune and epithelial cell types from bulk tissue RNA-seq data, revealed cell type-specific effects of HM exposures. For instance, the decrease in alveolar epithelial type 1 cells and increase in B cells following  $\text{NaAsO}_2$  exposure aligns with known effects of arsenic on epithelial damage and immune cell recruitment. Similarly, the increased monocyte populations in  $\text{MnCl}_2$ -exposed tissues reflect



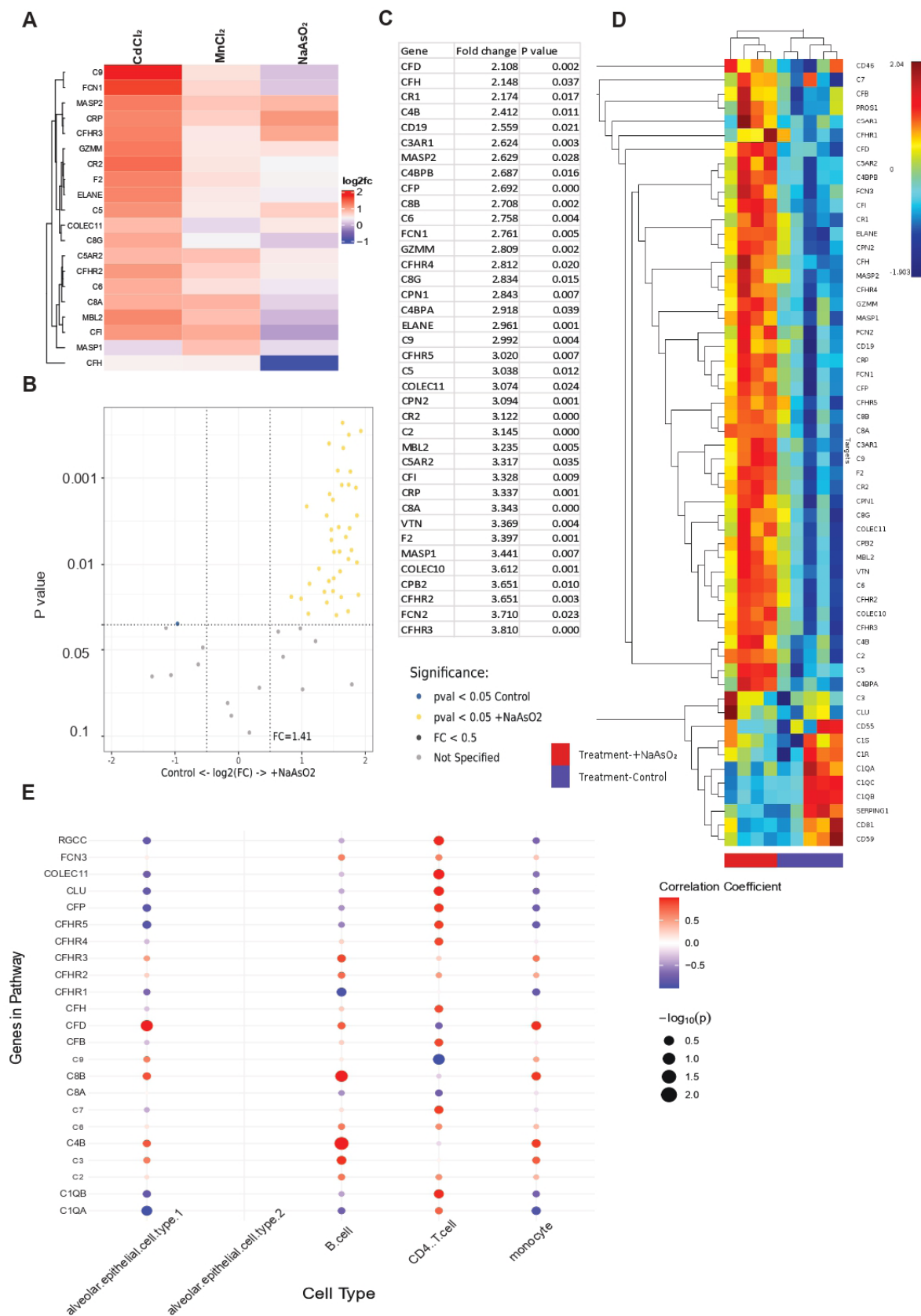


**Figure 2.** Gene expression changes in the complement pathway in HM-exposed lung tissues. A. Heatmap showing gene expression of complement pathway genes following CdCl<sub>2</sub>, MnCl<sub>2</sub>, or NaAsO<sub>2</sub> exposure normalized to unexposed controls. B-C. Table (B) and heatmap (C) highlighting significantly altered genes with NaAsO<sub>2</sub> exposure. D. Volcano plot displaying differential gene expression between NaAsO<sub>2</sub>-exposed and unexposed (control) lung tissues. E. Cell deconvolution analysis correlating gene expression of complement pathway with scaled abundance of specific cell populations in the lung tissue following NaAsO<sub>2</sub> exposure.

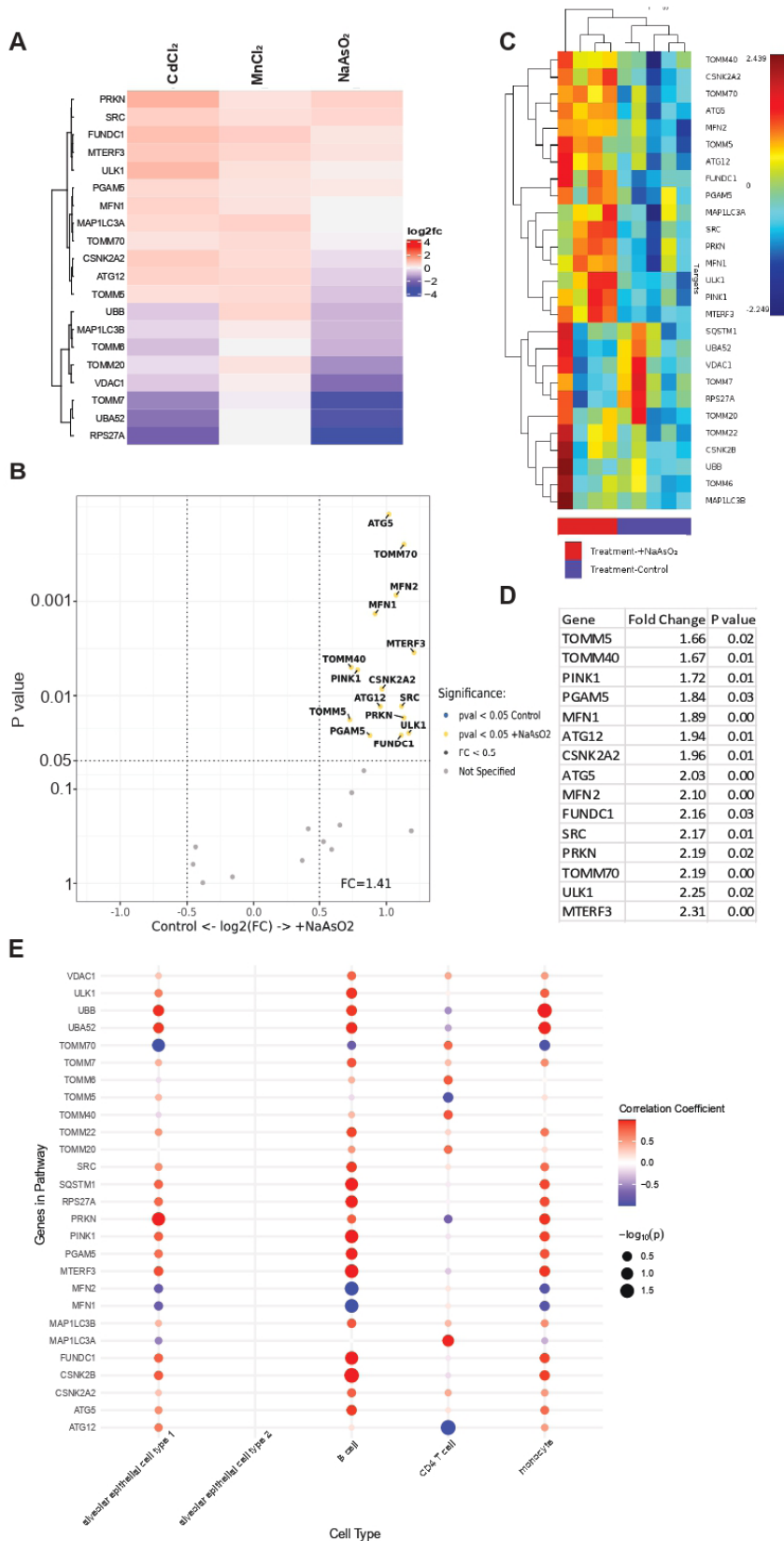


**Figure 3.** Gene expression changes in the mitophagy pathway in HM-exposed lung tissues. A. Heatmap showing gene expression of mitophagy pathway genes following CdCl<sub>2</sub>, MnCl<sub>2</sub>, or NaAsO<sub>2</sub> exposure normalized to unexposed controls. B-C. Table (B) and heatmap (C) highlighting significantly altered genes with NaAsO<sub>2</sub> exposure. D. Volcano plot displaying differential gene expression between NaAsO<sub>2</sub>-exposed and unexposed (control) lung tissues. E. Cell deconvolution analysis correlating gene expression of mitophagy with scaled abundance of specific cell populations in the lung tissue following NaAsO<sub>2</sub> exposure.

monocyte-mediated inflammation.

The positive correlations between sphingolipid metabolism gene upregulation and certain immune cell populations (B cells, monocytes, CD4<sup>+</sup> T cells) suggest that sphingolipid dysregulation may modulate or be modulated by immune cell infiltration and activation, contributing to the inflammatory milieu in HM-exposed lung tissue. These cell-specific associations further support the hypothesis that sphingolipid metabolism alterations underlie inflammatory signaling pathways involved in lung disease pathogenesis following HM exposure.

Overall, the integrated approach combining transcriptional profiling with cell type deconvolution provides a robust framework to elucidate how environmental HMs disrupt sphingolipid metabolism in a cell-specific manner, contributing to lung tissue inflammation and remodeling characteristic of chronic respiratory diseases.

During chronic inflammation, oxidative stress induces activation of complement cascade leading to tissue injury [39,40]. Sphingolipid metabolites can also directly influence complement cascade activation that may bridge innate and adaptive immune responses [41]. As NaAsO<sub>2</sub> modulated gene signatures of sphingolipid metabolism in both innate and adaptive immune cells, we evaluated HM-induced alterations in components of the complement cascade. As shown in Figure 2A (Supplemental Table 1), clustered heatmap analyses of exposed tissues compared to unexposed controls revealed differential increase in complement cascade genes amongst the three heavy metals. Although the highest fold change occurred in the CdCl<sub>2</sub> exposed tissues, volcano plot and clustered heatmap analyses identified substantially more complement pathway genes upregulated in the NaAsO<sub>2</sub>-treated tissues (Figure 2B-D). Intersecting alterations in gene signatures were noted with MASP1, MBL2, C8A and CFI significantly upregulated following both NaAsO<sub>2</sub> and MnCl<sub>2</sub> exposure (Figure 2B and Supplemental Figure 4A). Notably, genes upregulated by NaAsO<sub>2</sub> exposure exhibited a higher fold change (~3) compared to MnCl<sub>2</sub> (~1.5). Conversely, ELANE, CR1, GZMM and C9 were significantly upregulated in both the NaAsO<sub>2</sub> and CdCl<sub>2</sub> exposed tissues, which displayed similar fold-change levels (Figure 2B and Supplemental Figure 5A).

We then investigated whether the HM-induced gene signatures of complement cascade correlated with cell populations in the exposed lung tissues. In tissues exposed to NaAsO<sub>2</sub>, complement cascade genes positively correlated with CD4<sup>+</sup> T cells and B cells, type I alveolar epithelial cells and monocytes, unlike MnCl<sub>2</sub> and CdCl<sub>2</sub> in which this pathway positively correlated primarily with alveolar epithelial cells (Figure 2E and Supplemental Figure 4C and 5C).

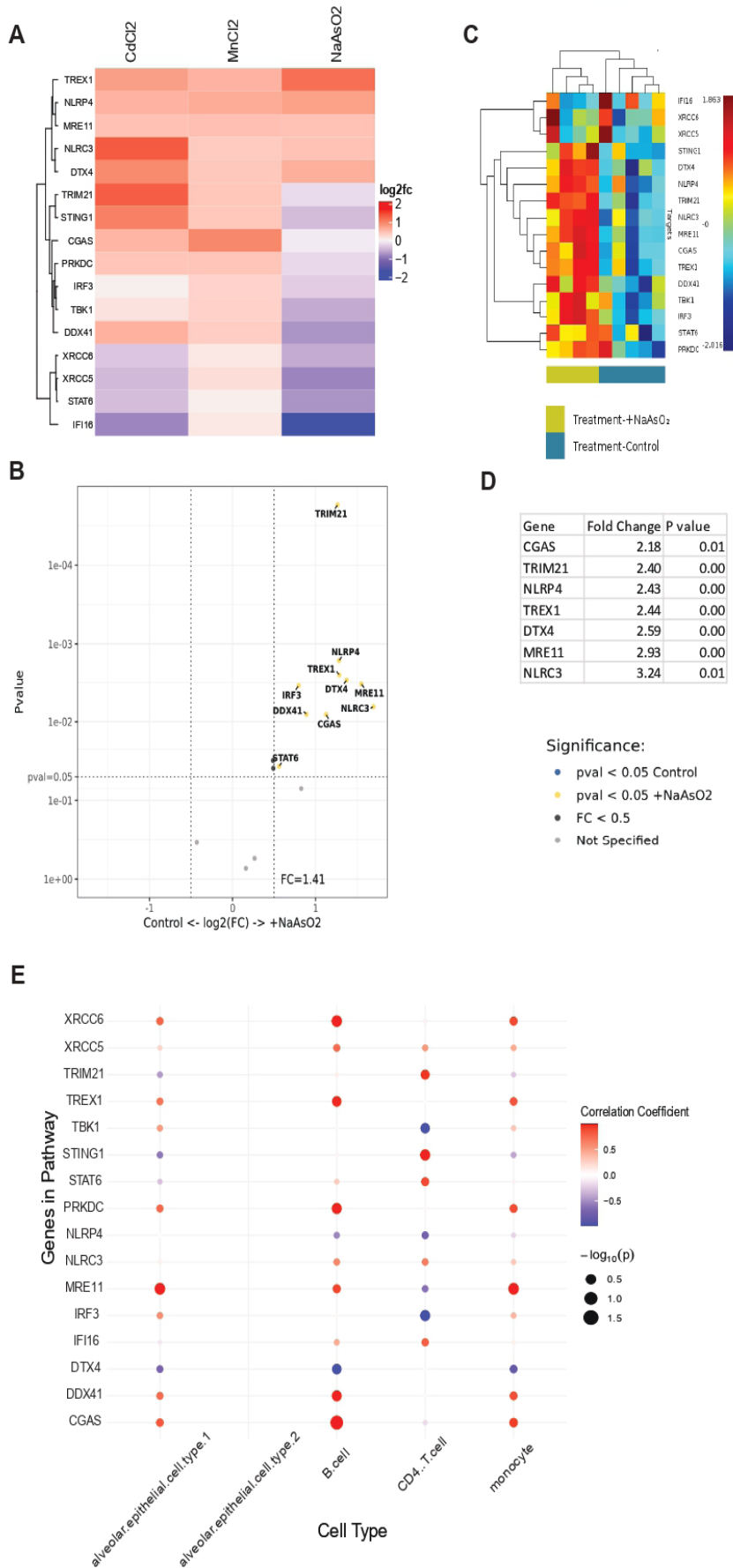
As complement cascade activation can trigger mitophagy during inflammation, we then investigated HM-induced changes in gene signatures of the mitophagy pathway [42]. Clustered heat map analyses of exposed tissues compared to unexposed controls highlighted differential increase in fold changes in mitophagy genes amongst three HMs (Figure 3A, Supplemental Table 1). Although the overall gene expression appears to be downregulated in NaAsO<sub>2</sub> compared to other two HMs, volcano plot and clustered heatmap analyses indicated that signifi-

cantly more number of mitophagy genes were upregulated in the NaAsO<sub>2</sub>-treated tissues compared to other HMs (Figure 3B-D, Supplemental Figures 6A-B and 7A-B). Following CdCl<sub>2</sub> exposure, only MAP1LC3A, was significantly altered, and no genes showed significant differential expression following MnCl<sub>2</sub> exposure. (Supplemental Figures 6A-B, 5D and 7A-B). We then correlated abundance score of cell populations within the exposed lung tissues and the HM-induced gene signatures related to mitophagy. In NaAsO<sub>2</sub>-exposed tissues, mitophagy pathway genes positively correlated with abundance scores of B cells and monocytes and type I alveolar epithelial cells (Figure 3D). Conversely, in MnCl<sub>2</sub> exposed tissues, positive correlation of this pathway was observed in only monocytes and type I alveolar epithelial cells, and in CdCl<sub>2</sub> exposure correlation was primarily with type I alveolar epithelial cells (Supplemental Figures 6C and 7C).

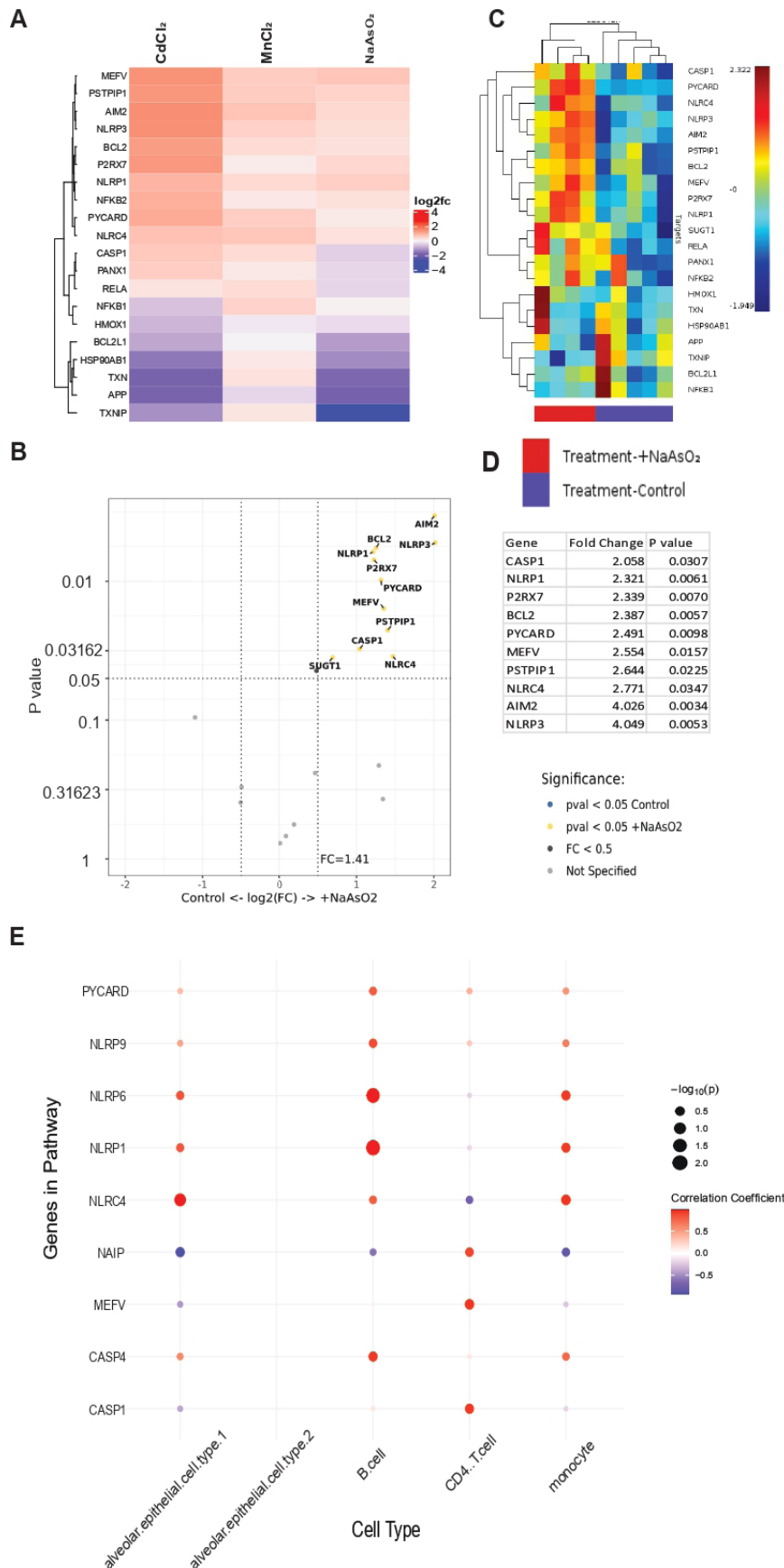
As mitophagy acts as a negative regulator of STING activation by preventing the release of mitochondrial DNA [43], and consequent DNA sensing, we investigated if gene signatures of STING pathway were affected by HM-exposure. As shown in Figure 4A and Supplemental Table 1, clustered heat map analyses of exposed tissues revealed differential increase in fold changes in STING pathway genes amongst three HMs when compared to unexposed controls. Although the highest fold change occurred in CdCl<sub>2</sub> exposed tissues, volcano plot and clustered heatmap analyses revealed that the dysregulated gene expression was significant only in the NaAsO<sub>2</sub>-treated tissues (Figure 4B-D, Supplemental Figures 8A-B and 9A-B). We then investigated whether the HM-induced gene signatures of STING pathway correlated with cell populations in the exposed lung tissues. In tissues exposed to NaAsO<sub>2</sub>, this pathway positively correlated primarily with abundance scores of B cells, with some correlation to type I alveolar epithelial cells, CD4<sup>+</sup> T cells, and monocytes. However, in MnCl<sub>2</sub>-exposed tissues, positive correlation was only observed in monocytes and type I alveolar epithelial cells, and CdCl<sub>2</sub> exposure was primarily correlated with type I alveolar epithelial cells (Supplemental Figures 8C and 9C).

Figure 4 Gene expression changes in the STING pathway in HM-exposed lung tissues. A. Heatmap showing gene expression of STING pathway genes following CdCl<sub>2</sub>, MnCl<sub>2</sub>, or NaAsO<sub>2</sub> exposure normalized to unexposed controls. B-C. Table (B) and heatmap (C) highlighting significantly altered genes with NaAsO<sub>2</sub> exposure. D. Volcano plot displaying differential gene expression between NaAsO<sub>2</sub>-exposed and unexposed (control) lung tissues. E. Cell deconvolution analysis correlating gene expression of STING pathway with scaled abundance of specific cell populations in the lung tissue following NaAsO<sub>2</sub> exposure.

Because STING activation initiates the induction of the inflammasome pathway and inflammasome induction is associated with chronic inflammatory lung diseases [16,32], we investigated whether inflammasome pathway genes were altered following HM-exposure. Clustered heat map analyses showed differential increase in fold changes in inflammasome genes amongst three HMs (Figure 5A, Supplemental Table 1). Although the highest fold change in expression of gene signatures occurred in the CdCl<sub>2</sub> exposed tissues, volcano plot and



**Figure 4.** Gene expression changes in the STING pathway in HM-502 exposed lung tissues. A. Heatmap showing gene expression of STING pathway genes following CdCl<sub>2</sub>, MnCl<sub>2</sub>, or NaAsO<sub>2</sub> exposure normalized to unexposed controls. B-C. Table (B) and heatmap (C) highlighting significantly altered genes with NaAsO<sub>2</sub> exposure. D. Volcano plot displaying differential gene expression between NaAsO<sub>2</sub>-exposed and unexposed (control) lung tissues. E. Cell deconvolution analysis correlating gene expression of STING pathway with scaled abundance of specific cell populations in the lung tissue following NaAsO<sub>2</sub> exposure.



**Figure 5.** Gene expression changes in the inflammasome activation pathway in HM exposed lung tissues. A. Heatmap showing gene expression of inflammasome activation pathway genes following CdCl<sub>2</sub>, MnCl<sub>2</sub>, or NaAsO<sub>2</sub> exposure normalized to unexposed controls. B-C. Table (B) and heatmap (C) highlighting significantly altered genes with NaAsO<sub>2</sub> exposure. D. Volcano plot displaying differential gene expression between NaAsO<sub>2</sub>-exposed and unexposed (control) lung tissues. E. Cell deconvolution analysis correlating gene expression of inflammasome activation with scaled abundance of specific cell populations in the lung tissue following NaAsO<sub>2</sub> exposure.

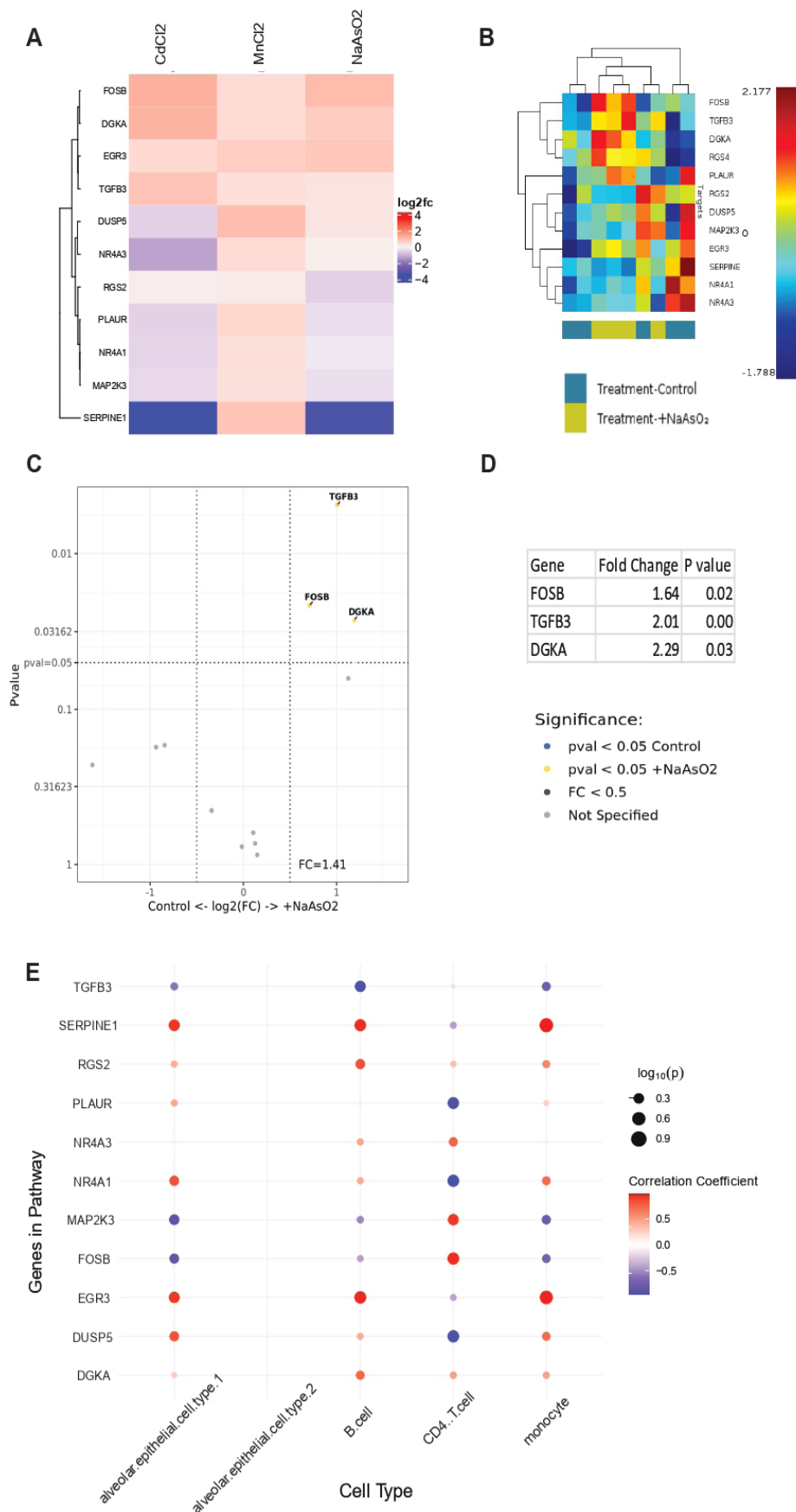


**Figure 6.** Gene expression changes in the airway remodeling pathway in HM-exposed lung tissues. A. Heatmap showing gene expression of airway remodeling pathway genes following CdCl<sub>2</sub>, MnCl<sub>2</sub>, or NaAsO<sub>2</sub> exposure. B-C. Table (B) and heatmap (C) highlighting significantly altered genes with NaAsO<sub>2</sub> exposure. D. Volcano plot displaying differential gene expression between NaAsO<sub>2</sub>-exposed and unexposed (control) lung tissues. E. Cell deconvolution analysis correlating gene expression of airway remodeling pathway with scaled abundance of specific cell populations in the lung tissue following NaAsO<sub>2</sub> exposure.

clustered heatmap analyses indicated that NaAsO<sub>2</sub>-treated tissues had considerably increased number of upregulated genes (Figure 5B-D, Supplemental Figures 10A-B, 10D, and 11A-B). Following CdCl<sub>2</sub> exposure, only MEFV, was significantly dysregulated, following MnCl<sub>2</sub> exposure. (Supplemental Figures 10A-B, 10D and 11A-B). Next, we investigated whether HM-induced inflammasome gene signatures correlated with cell abundance. In tissues exposed to NaAsO<sub>2</sub>, a positive correlation of inflammasome-related genes was observed with B cells with some correlation to type I alveolar epithelial cells, CD4<sup>+</sup>T cells, and monocytes. However, in MnCl<sub>2</sub>-exposed tissues, positive correlation was only observed in monocytes and type I alveolar epithelial cells, and gene changes with CdCl<sub>2</sub> exposure correlated primarily with alveolar epithelial Type I cells (Supplemental Figures 10C and 11C).

Environmental exposures are known to contribute to airway remodeling in chronic inflammatory lung diseases [9,44]. Therefore, we investigated if airway remodeling genes were altered by HM-exposure in exposed lung tissues. Clustered heat map analyses emphasized differential increase in fold changes in airway remodeling genes amongst three heavy metals (Figure 6A, Supplemental Table 1). Although the highest fold change in expression of gene signatures occurred in the MnCl<sub>2</sub> exposed tissues, volcano plot and clustered heatmap analyses indicated that airway remodeling genes were significantly upregulated in only NaAsO<sub>2</sub>-treated tissues (Figure 6B-D, Supplemental Figures 12A-B and 13A-B). In tissues exposed to NaAsO<sub>2</sub>, correlation of altered gene signatures with cell deconvolution showed that this pathway correlated positively with monocytes and B cells, along with some correlation with CD4<sup>+</sup> T cells and type I alveolar epithelial cells, as seen in Figure 6E. However, in MnCl<sub>2</sub> exposed tissues, these gene signatures positively correlated with cell abundance scores of monocytes and type I alveolar epithelial cells, and in CdCl<sub>2</sub> exposure, positive correlation was primarily with type I alveolar epithelial cells (Supplemental Figure 12C and 13C).

We then evaluated pairwise correlation between gene signatures of these pathways following NaAsO<sub>2</sub> exposure. Gene expression in the complement pathway is regulated by sphingolipid metabolism genes through crosstalk between pro-survival sphingolipid signaling and complement activation [45]. Consistent with this, expression of the complement genes C8A, C8B, C9, CD46, CD55, and CD59 were significantly correlated with the expression of the sphingolipid metabolism genes CERS5, CERS4, ARSF, and ARSD (Supplemental Figure 14). Expression of complement genes C1QA, C1QB, C1QC, C5, C6C8G, CD81, CFB, CFH and CFHR4 are significantly correlated with sphingolipid genes UGCG, SUMF1, STS, SMPD4, PRKD2, PPM1L, HEXB, GM2A, ESYT2, and DEGS2 (Supplemental Figure 14).

We then investigated the relationship between gene expression changes in sphingolipid metabolism, STING, mitophagy, and the inflammasome pathway. Pairwise correlation analyses showed that the expression of the sphingolipid genes ARSF, CERS4, CERS5, GBA, HEXA, KDSR, PRKD1, and SPTLC1 significantly correlated with the inflammasome genes NFKB1 and MEFV (Supplemental Figure 15A); expression of mitoph-

agy genes ATG12, MFN2, PRKN, TOMM20, and UBA52 significantly correlated with the expression of sphingolipid genes ARSD, ARSF, CERS4, CERS5, GBA, ORMDL2, PRKD1, SPTLC1, and SPTSSB (Supplemental Figure 15B). Expression of STING pathway genes IFI16, IRF3, STING1, and TBK1 significantly correlated with the expression of the sphingolipid genes ARSD, ARSF, CERS4, CERS5, HEXA, and KDSR (Supplemental Figure 15C), while NLRP4, STAT6, and TRIM21 significantly correlated with the expression of the sphingolipid genes DEGS2, ESYT2, GM2A, HEXB, PPM1L, PRKD2, PRKD3, SMPD4, SPTSSA, and SUMF1 (Supplemental Figure 15C). Pairwise correlation of expression of STING pathway genes IFI16, IRF3, NLRC3, and STING1 with inflammasome pathway genes MEFV and NFKB1 (Supplemental Figure 15D) was noted. A different set of STING pathway genes IFI16, STAT6, and TBK1 significantly correlated with the inflammasome gene AIM2 (Supplemental Figure 15D); while NLRC3 and STING1 significantly correlated with ATG12, ATG5, MFN2, TOMM20, TOMM7, and UBA52 (Supplemental Figure 15E), and IFI16 and IRF3 significantly correlated with ATG12, MFN2, PRKN, TOMM20, and UBA52 (Supplemental Figure 15E).

Pairwise correlations of the complement, mitophagy, STING, and inflammasome pathways revealed parallels in gene regulation. Expression of complement genes C1R, C8B, CD46, CD55, CD59, CFHR2, CPN2, F2, and SERPING2 significantly correlated with expression of the mitophagy pathway genes ATG12, ATG5, MFN2, PRKN, TOMM20, UBA52 (Supplemental Figure 16A); complement genes C8B, CD46, CD55, CD59, CFHR2, CPN2, and F2 significantly correlated with expression of inflammasome pathway genes MEFV and NFKB1. A different set of complement genes C1R, C2, C4BPB, C8A, C9, CFD significantly correlated with expression of the inflammasome pathway gene AIM2 (Supplemental Figure 16B). Expression of complement genes C1R, C8B, CD46, CD55, CD59, CFD, CFHR2, CPN2, and SERPING2 are significantly correlated with STING genes IFI16, IRF3, and TBK1 (Supplemental Figure 16C). When correlating the mitophagy and the inflammasome pathways, the expression of the mitophagy genes ATG12, ATG5, MAP1LC3, MFN2, PRKN, TOMM20, TOMM7, and UBA52 are significantly correlated with the expression of the inflammasome genes NFKB1 and MEFV (Supplemental Figure 16D).

The airway remodeling pathway genes also displayed pairwise correlation with gene signatures of mitophagy, inflammasome, complement, and sphingolipid pathway. When correlating sphingolipid metabolism gene expression with airway remodeling gene expression, sphingolipid genes ALDH3A2, ARSD, ASAH1, CERS2, PLPP2, PRKD3, SPTSSB, and SUMF2 are significantly correlated with airway remodeling genes NR4A3, PLAUR, RGS2, and SERPINE1 (Supplemental Figure 17A). Expression of the complement genes C1R, C2, C4BPB, C8A, C9, and CFD are significantly correlated with airway remodeling genes NR4A3, PLAUR, RGS2, and SERPINE1 (Supplemental Figure 17B); CFH and CFB also significantly correlated with airway remodeling genes PLAUR and RGS2 (Supplemental Figure 17B). Expression of the airway remodeling gene DUSP5

significantly correlated with the mitophagy genes ATG12, ATG5, MFN2, PRKN, TOMM20, and UBA52 (Supplemental Figure 17C), while NR4A3, PLAUR, RGS2, and SERPINE1 significantly correlated with the mitophagy genes PRKN and TOMM5 (Supplemental Figure 17C). Expression of the airway remodeling genes DUSP5 and NR4A3 significantly correlated with expression of the STING genes IFI16, IRF3, and TBK1, while NR4A3, PLAUR, RGS2, and SERPINE1 significantly correlated with the expression of STING genes STING1 and TBK1 (Supplemental Figure 17D). Expression of the inflammasome genes BCL2L1, PANX1, and PSTPIP1 also significantly correlated with the airway remodeling gene TGFB3 (Supplemental Figure 17E), while AIM2, significantly correlated with the airway remodeling genes SERPINE1, RGS2, PLAUR, NR4A3 (Supplemental Figure 17E).

## Discussion

We have previously reported that HM exposures result in differential expression of oxidative stress gene signatures of inflammatory signaling and expression of the sphingolipid enzymes SPHK1, CERS2, and ORMDL3 that alter sphingolipid homeostasis in both human lung epithelial cells and human lung tissues. These inflammatory signaling and sphingolipid pathway alterations are known to play an important role in sustaining the inflammatory response in asthma [38]. Consistent with our previous report, our current spatial transcriptomics studies show that gene signatures associated with sphingolipid metabolism were upregulated following HM exposure, with NaAsO<sub>2</sub> exposure being the most impactful. Additionally, we report changes in gene signatures of complement cascade, downstream innate immune signaling pathways and airway remodeling genes that correlated with transcriptional alterations in sphingolipid metabolism pathway. These data suggest that sphingolipid metabolism is dysregulated following HM exposure, and may contribute to chronic inflammatory lung diseases including asthma [37].

As oxidative stress induces activation of complement cascade leading to tissue injury [39,40] and complement activation is known to bridge the innate and adaptive immune response, we evaluated the effects of HM-exposure on complement cascade; three different pathways-classical, alternative, or leptin-can activate this signaling cascade using either innate or adaptive components. We report a novel link between HM exposures and complement cascade activation, with NaAsO<sub>2</sub> exposure resulting in substantial upregulation of complement genes with highest fold changes with this HM exposure. The activation of complement pathway can stimulate TH2-mediated inflammatory responses via the complement component C3a, which is responsible for mast cell activation and smooth muscle contraction, commonly associated with asthmatic responses [34,35]. Other complement components, such as C5 and Factor H, may also influence asthma pathophysiology by aggravating T-helper type 2 (TH2) immune response and airway AHR in an allergic murine model of asthma [46]. The generation of C5a contributed to TH2 differentiation without impacting innate lymphoid cells in a house dust mite murine asthma model [47]. Our transcriptomic studies showed significant upregulation of complement genes including C5 and Factor H following HM exposure. We also observed that the altered complement genes correlated with changes in sphingolip-

id pathway genes following NaAsO<sub>2</sub> exposure. Our observation that the upregulation of complement pathway correlated with inflammatory cell abundance scores of both innate cells, such as monocytes, and adaptive cells, such as CD4<sup>+</sup> T cells and B cells, suggests that the HM-exposure induced activation of complement pathway may play a role in the innate and adaptive immune responses associated with asthma.

The complement system uses pattern recognition receptors to detect damage-associated molecular patterns (DAMPs) released from injured or stressed cells, inducing intracellular signals [48]. When the mitochondria are injured, they secrete DAMPs and undergo mitophagy, a process by which autophagosomes remove dysfunctional mitochondria [49]. Our studies showed a significant upregulation of mitophagy genes following NaAsO<sub>2</sub>. We also observed a correlation between genes in the mitophagy and complement pathways. This suggests that mitophagy may activate the complement system, further attributing to asthma exacerbation. These results are consistent with previous reports that HM exposure can cause excessive ROS, and contribute to fibrosis in severe asthmatics [50,51]. ROS produced by oxidative phosphorylation are associated with mitophagy [52]. A similar pattern was seen in a murine model displaying ferroptosis, a form of cell death caused by excess iron, where cadmium exposure caused excessive mitophagy by upregulating Pink1 and Parkin, causing severe kidney damage [53]. Therefore, HM-exposure induced mitophagy has the potential to contribute to lung damage.

Oxidative stress-induced cell and tissue damage causes release of damaged DNA and activation of innate immune DNA sensing signaling pathways. In addition to mitophagy, genes associated with STING pathway, an innate immune signaling mechanism, were significantly upregulated following NaAsO<sub>2</sub> exposure and these gene expression changes were more robust with NaAsO<sub>2</sub> exposure than with the other two HMs. Previous studies of arsenic exposure in hepatocytes showed induction of mitochondrial DNA (mtDNA) leakage into the cytoplasm, leading to STING activation and subsequent increase in pro-inflammatory cytokines which may contribute to exacerbation of asthma following HM exposure [54]. Because STING activation can induce inflammasome pathway during HM-exposures [16], we examined inflammasome-related genes following NaAsO<sub>2</sub> exposure and found a substantial upregulation in gene expression when compared to the other two metals. A significant correlation between the complement and STING pathway genes was observed; similarly, a strong correlation was observed between mitophagy and inflammasome pathways. This finding aligns with a prior study demonstrating that arsenic exposure promotes NLRP3 inflammasome activation, contributing to systemic inflammation and metabolic dysfunction, in murine models [55]. Inflammasome activation also leads to the secretion of pro-inflammatory cytokines such as IL-1 $\beta$  and IL-18, which are implicated in asthma pathogenesis [55-57].

As these pathways associated with asthma pathogenesis were modulated, we evaluated whether this would impact genes involved with airway remodeling. Following NaAsO<sub>2</sub> exposure, significant upregulation of airway remodeling genes, FOSB, TGFB3, and DGKA, was observed. This is consistent with previous studies using a murine model of bronchial asthma follow-

ing arsenic exposure, which demonstrated that transforming growth factor  $\beta$ 1, vascular endothelial growth factor A, and matrix metalloproteinase-9 (MMP9) play key roles in chronic asthma-genes that can be influenced by the expression of FOSB and TGFB3 [58,59]. MMP9 can be affected by FOSB. The airway remodeling pathway exhibited significant pairwise correlations with the sphingolipid, complement, STING, and mitophagy pathway, suggesting that these pathways may be linked with asthma pathogenesis via their relationship with airway remodeling. Taken together, our results suggest that HM-induced oxidative stress drives multiple inflammatory and remodeling pathways and has the potential to exacerbate asthma through immune activation and airway structural alterations.

This study provides novel evidence linking HM exposure to complement activation and, ultimately, having the potential to cause asthma exacerbation by modulation of inflammatory signaling. It corroborates previous findings on the role of HM exposure in inducing mitophagy, inflammasome activation, STING signaling, and airway remodeling pathways through gene expression analysis. However, despite using human lung samples, this study does not address *in vivo* validation in human subjects and does not establish how these specific gene expression changes translate into the physiological manifestations of asthma.

#### Author contributions

S.L.S. was involved in data collection, data analysis, and manuscript and figure preparation. K.P.H. was involved in data analysis. S.S. was involved in data collection and figure editing. M.A. provided critical assessment of the manuscript and provided expertise in HM exposure studies. K.F.G. was involved in experimental execution, data collection, data analysis, and oversight. J.S.D. was involved in experimental design and oversight, data interpretation, and gave critical insights on the manuscript. All authors have read and agreed to the published version of manuscript.

#### Funding

This research was supported NIEHS P42 Project 2 (ES027723), NCI (1R21 CA263365-01A1) and pilot award from School of Medicine, University of Alabama at Birmingham, all awarded to J.S.D.

#### Institutional review board statement

Human tissue collection for this study occurred under an Institutional Review Board of the University of Alabama at Birmingham approved protocol (IRB-300003092) which was approved as Not Human Subjects Research.

#### Informed consent statement

Remnant surgical specimens were collected through the Institutional UAB Tissue Biorepository's waiver of informed consent and no identifying information was provided.

#### Data availability statement

The original data presented in the study are openly available in GEO (GSE297051).

#### Acknowledgments

We acknowledge the UAB Tissue Biorepository, the UAB

Pathology Research Core, the UAB Spatial Profiling and Transplant Immuno-Assay Laboratory (SPATIAL) Core, and the UAB Genomics Core Facilities for their support in performing experiments.

#### Conflicts of Interest

K.F.G. and J.S.D. are equal partners of Dynamic Tissue Mimics, LLC which has not yielded revenue.

#### References

1. Protection CD. Particulate Matter Fact Sheet. Available from: <https://portal.ct.gov/deep/air/planning/particulate-matter/particulate-matter-fact-sheet>. Accessed 2024 Oct 7.
2. United States Environmental Protection Agency. Particulate Matter (PM) Basics. Available from: <https://www.epa.gov/pm-pollution/particulate-matter-pm-basics>. Accessed 2024 Oct 7.
3. Dunea D, Iordache S, Liu HY, Bohler T, Pohoata A, Radulescu C, et al. Quantifying the impact of PM2.5 and associated heavy metals on respiratory health of children near metallurgical facilities. *Environ Sci Pollut Res Int*. 2016;23(15):15395–406. doi:10.1007/s11356-016-6734-x.
4. Zeng X, Xu X, Qin Q, Ye K, Wu W, Huo X, et al. Heavy metal exposure has adverse effects on the growth and development of preschool children. *Environ Geochem Health*. 2019;41(1):309–21. doi:10.1007/s10653-018-0114-z.
5. Cachon BF, Firmin S, Verdin A, Ayi-Fanou L, Billet S, Cazier F, et al. Proinflammatory effects and oxidative stress within human bronchial epithelial cells exposed to atmospheric particulate matter (PM2.5 and PM>2.5) collected from Cotonou, Benin. *Environ Pollut*. 2014;185:340–51. doi:10.1016/j.envpol.2013.10.026.
6. Skalny AV, Lima TRR, Ke T, Zhou JC, Bornhorst J, Alekseenko SI, et al. Toxic metal exposure as a possible risk factor for COVID-19 and other respiratory infectious diseases. *Food Chem Toxicol*. 2020;146:111809. doi:10.1016/j.fct.2020.111809.
7. Salvi SS, Barnes PJ. Chronic obstructive pulmonary disease in non-smokers. *Lancet*. 2009;374(9691):733–43. doi:10.1016/S0140-6736(09)61303-9.
8. Mabalirajan U, Rehman R, Ahmad T, Kumar S, Singh S, Leishangthem GD, et al. Linoleic acid metabolite drives severe asthma by causing airway epithelial injury. *Sci Rep*. 2013;3:1349. doi:10.1038/srep01349.
9. Hough KP, Trevor JL, Strenkowski JG, Wang Y, Chacko BK, Toussif S, et al. Exosomal transfer of mitochondria from airway myeloid-derived regulatory cells to T cells. *Redox Biol*. 2018;18:54–64. doi:10.1016/j.redox.2018.06.009.
10. Qian L, Mehrabi Nasab E, Athari SM, Athari SS. Mitochondria Signaling Pathways in Allergic Asthma. *J Investig Med*. 2022;70(4):863–82. doi:10.1136/jim-2021-002098.
11. Morales ME, Derbes RS, Ade CM, Ortego JC, Stark J, Deininger PL, et al. Heavy Metal Exposure Influences Double Strand Break DNA Repair Outcomes. *PLoS One*. 2016;11(3):e0151367. doi:10.1371/journal.pone.0151367.
12. Du Y, Luo Y, Hu Z, Lu J, Liu X, Xing C, et al. Activation of cGAS-

- STING by Lethal Malaria N67C Dictates Immunity and Mortality through Induction of CD11b+ Ly6Chi Proinflammatory Monocytes. *Adv Sci (Weinh)*. 2022;9:e2103701. doi:10.1002/adv.202103701.
13. Hagiwara AM, Moore RE, Wallace DJ, Ishimori M, Jefferies CA. Regulation of cGAS-STING Pathway - Implications for Systemic Lupus Erythematosus. *Rheumatol Immunol Res*. 2021;2(4):173–84. doi:10.2478/rir-2021-0023.
  14. Han Y, Chen L, Liu H, Jin Z, Wu Y, Wu Y, et al. Airway epithelial cGAS is critical for induction of experimental allergic airway inflammation. *J Immunol*. 2020;204(6):1437–1447. doi:10.4049/jimmunol.1900869.
  15. Ishikawa H, Ma Z, Barber GN. STING regulates intracellular DNA-mediated, type I interferon-dependent innate immunity. *Nature*. 2009;461(7265):788–792. doi:10.1038/nature08476.
  16. Liu J, Zhang X, Wang H. The cGAS-STING-mediated NLRP3 inflammasome is involved in the neurotoxicity induced by manganese exposure. *Biomed Pharmacother*. 2022;154:113680. doi:10.1016/j.biopha.2022.113680.
  17. Ma R, Ortiz Serrano TP, Davis J, Prigge AD, Ridge KM. The cGAS-STING pathway: The role of self-DNA sensing in inflammatory lung disease. *FASEB J*. 2020;34(9):13156–13170. doi:10.1096/fj.202001607R.
  18. Ozasa K, Temizoz B, Kusakabe T, Kobari S, Momota M, Coban C, et al. Cyclic GMP-AMP triggers asthma in an IL-33-dependent manner that is blocked by Amlexanox, a TBK1 inhibitor. *Front Immunol*. 2019;10:2212. doi:10.3389/fimmu.2019.02212.
  19. Zhang X, Liu J, Wang H. The cGAS-STING-autophagy pathway: Novel perspectives in neurotoxicity induced by manganese exposure. *Environ Pollut*. 2022;315:120412. doi:10.1016/j.envpol.2022.120412.
  20. Ning L, Wei W, Wenyang J, Rui X, Qing G. Cytosolic DNA-STING-NLRP3 axis is involved in murine acute lung injury induced by lipopolysaccharide. *Clin Transl Med*. 2020;10(5):e228. doi:10.1002/ctm2.228.
  21. Chan TK, Loh XY, Peh HY, Tan WNF, Tan WSD, Li N, et al. House dust mite-induced asthma causes oxidative damage and DNA double-strand breaks in the lungs. *J Allergy Clin Immunol*. 2016;138(1):84–96.e1. doi:10.1016/j.jaci.2016.02.017.
  22. Hoshino T, Okamoto M, Takei S, Sakazaki Y, Iwanaga T, Aizawa H. Redox-regulated mechanisms in asthma. *Antioxid Redox Signal*. 2008;10(4):769–783. doi:10.1089/ars.2007.1936.
  23. Hosoki K, Chakraborty A, Hazra TK, Sur S. Protocols to measure oxidative stress and DNA damage in asthma. *Methods Mol Biol*. 2022;2506:315–332. doi:10.1007/978-1-0716-2364-0\_22.
  24. Jarjour NN, Calhoun WJ. Enhanced production of oxygen radicals in asthma. *J Lab Clin Med*. 1994;123(1):131–136.
  25. Zahiruddin AS, Grant JA, Sur S. Role of epigenetics and DNA-damage in asthma. *Curr Opin Allergy Clin Immunol*. 2018;18(1):32–37. doi:10.1097/ACI.0000000000000415.
  26. Burdette DL, Monroe KM, Sotelo-Troha K, Iwig JS, Eckert B, Hyodo M, et al. STING is a direct innate immune sensor of cyclic di-GMP. *Nature*. 2011;478(7370):515–518. doi:10.1038/nature10429.
  27. Sharma A, Ahmad S, Ahmad T, Ali S, Syed MA. Mitochondrial dynamics and mitophagy in lung disorders. *Life Sci*. 2021;284:119876. doi:10.1016/j.lfs.2021.119876.
  28. Li R, Kou X, Geng H, Xie J, Yang Z, Zhang Y, et al. Effect of ambient PM<sub>2.5</sub> on lung mitochondrial damage and fusion/fission gene expression in rats. *Chem Res Toxicol*. 2015;28(3):408–418. doi:10.1021/tx5003723.
  29. Wang HT, Lin JH, Yang CH, Haung CH, Weng CW, Lin AMY, et al. Acrolein induces mtDNA damages, mitochondrial fission and mitophagy in human lung cells. *Oncotarget*. 2017;8(44):70406–70421. doi:10.18632/oncotarget.19710.
  30. Duncan JA, Bergstralh DT, Wang Y, Willingham SB, Ye Z, Zimmermann AG, et al. Cryopyrin/NALP3 binds ATP/dATP, is an ATPase, and requires ATP binding to mediate inflammatory signaling. *Proc Natl Acad Sci U S A*. 2007;104(19):8041–8046. doi:10.1073/pnas.0611496104.
  31. Zheng R, Tao L, Jian H, Chang Y, Cheng Y, Feng Y, et al. NLRP3 inflammasome activation and lung fibrosis caused by airborne fine particulate matter. *Ecotoxicol Environ Saf*. 2018;163:612–619. doi:10.1016/j.ecoenv.2018.07.076.
  32. Theofani E, Semitekoulou M, Morianos I, Samitas K, Xanthou G. Targeting NLRP3 inflammasome activation in severe asthma. *J Clin Med*. 2019;8(10):1615. doi:10.3390/jcm8101615.
  33. Choi MS, Jeon H, Yoo SM, Lee MS. Activation of the complement system on human endothelial cells by urban particulate matter triggers inflammation-related protein production. *Int J Mol Sci*. 2021;22(6):3336. doi:10.3390/ijms22063336.
  34. Wills-Karp M. Complement activation pathways: a bridge between innate and adaptive immune responses in asthma. *Proc Am Thorac Soc*. 2007;4(3):247–251. doi:10.1513/pats.200704-046AW.
  35. Kokelj S, Ostling J, Fromell K, Vanfleteren L, Olsson HK, Nilsson Ek Dahl K, et al. Activation of the complement and coagulation systems in the small airways in asthma. *Respiration*. 2023;102(8):621–631. doi:10.1159/000531374.
  36. Vedel-Krogh S, Rasmussen KL, Nordestgaard BG, Nielsen SF. Complement C3 and allergic asthma: a cohort study of the general population. *Eur Respir J*. 2021;57(4):200645. doi:10.1183/13993003.00645-2020.
  37. Kowal K, Zebrowska E, Chabowski A. Altered sphingolipid metabolism is associated with asthma phenotype in house dust mite-allergic patients. *Allergy Asthma Immunol Res*. 2019;11(3):330–342. doi:10.4168/aa.2019.11.3.330.
  38. Ahmad S, Single S, Liu Y, Hough KP, Wang Y, Thannickal VJ, et al. Heavy metal exposure-mediated dysregulation of sphingolipid metabolism. *Antioxidants (Basel)*. 2024;13(8):978. doi:10.3390/antiox13080978.
  39. Collard CD, Vakeva A, Morrissey MA, Agah A, Rollins SA, Reenstra WR, et al. Complement activation after oxidative stress: role of the lectin complement pathway. *Am J Pathol*. 2000;156(5):1549–1556. doi:10.1016/S0002-9440(10)65026-2.
  40. Tezel G, Yang X, Luo C, Kain AD, Powell DW, Kuehn MH, et al. Oxidative stress and the regulation of complement activation in human glaucoma. *Invest Ophthalmol Vis Sci*. 2010;51(10):5071–

5082. doi:10.1167/iov.10-5289.
41. Bachmaier K, Guzman E, Kawamura T, Gao X, Malik AB. Sphingosine kinase 1 mediation of expression of the anaphylatoxin receptor C5L2 dampens the inflammatory response to endotoxin. *PLoS One*. 2012;7(2):e30742. doi:10.1371/journal.pone.0030742.
  42. Nguyen H, Kuril S, Bastian D, Kim J, Zhang M, Vaena SG, et al. Complement C3a and C5a receptors promote GVHD by suppressing mitophagy in recipient dendritic cells. *JCI Insight*. 2018;3(15):e121697. doi:10.1172/jci.insight.121697.
  43. Zhong W, Rao Z, Xu J, Sun Y, Hu H, Wang P, et al. Defective mitophagy in aged macrophages promotes mitochondrial DNA cytosolic leakage to activate STING signaling during liver sterile inflammation. *Aging Cell*. 2022;21(5):e13622. doi:10.1111/ace1.13622.
  44. Scott JA, Grasemann H. Arginine metabolism in asthma. *Immunol Allergy Clin North Am*. 2014;34(4):767–775. doi:10.1016/j.ia.2014.07.007.
  45. Janneh AH, Kassir MF, Atilgan FC, Lee HG, Sheridan M, Oleinik N, et al. Crosstalk between pro-survival sphingolipid metabolism and complement signaling induces inflammasome-mediated tumor metastasis. *Cell Rep*. 2022;41(6):111742. doi:10.1016/j.celrep.2022.111742.
  46. Tornyi I, Horvath I. Role of complement components in asthma: a systematic review. *J Clin Med*. 2024;13(11):3044. doi:10.3390/jcm13113044.
  47. Yang J, Ramirez Moral I, van 't Veer C, de Vos AF, de Beer R, Roelofs J, et al. Complement factor C5 inhibition reduces type 2 responses without affecting group 2 innate lymphoid cells in a house dust mite induced murine asthma model. *Respir Res*. 2019;20(1):165. doi:10.1186/s12931-019-1136-5.
  48. Hess C, Kemper C. Complement-mediated regulation of metabolism and basic cellular processes. *Immunity*. 2016;45(2):240–254. doi:10.1016/j.immuni.2016.08.003.
  49. Mohamud Y, Xue YC, Liu H, Ng CS, Bahreyni A, Luo H, et al. Autophagy receptor protein Tax1-binding protein 1/TRAF6-binding protein is a cellular substrate of enteroviral proteinase. *Front Microbiol*. 2021;12:647410. doi:10.3389/fmicb.2021.647410.
  50. Ramakrishnan RK, Bajbouj K, Hachim MY, Mogas AK, Mahboub B, Olivenstein R, et al. Enhanced mitophagy in bronchial fibroblasts from severe asthmatic patients. *PLoS One*. 2020;15(11):e0242695. doi:10.1371/journal.pone.0242695.
  51. Fan X, Dong T, Yan K, Ci X, Peng L. PM2.5 increases susceptibility to acute exacerbation of COPD via NOX4/Nrf2 redox imbalance-mediated mitophagy. *Redox Biol*. 2023;59:102587. doi:10.1016/j.redox.2022.102587.
  52. Ornatowski W, Lu Q, Yegambaram M, Garcia AE, Zemskov EA, Maltepe E, et al. Complex interplay between autophagy and oxidative stress in the development of pulmonary disease. *Redox Biol*. 2020;36:101679. doi:10.1016/j.redox.2020.101679.
  53. Qiu W, Ye J, Su Y, Zhang X, Pang X, Liao J, et al. Co-exposure to environmentally relevant concentrations of cadmium and polystyrene nanoplastics induced oxidative stress, ferroptosis and excessive mitophagy in mice kidney. *Environ Pollut*. 2023;333:121947. doi:10.1016/j.envpol.2023.121947.
  54. Pan H, Su Q, Hong P, You Y, Zhou L, Zou J, et al. Arsenic-induced mtDNA release promotes inflammatory responses through cGAS-STING signaling in chicken hepatocytes. *Pestic Biochem Physiol*. 2024;205:106129. doi:10.1016/j.pestbp.2024.106129.
  55. Jia X, Qiu T, Yao X, Jiang L, Wang N, Wei S, et al. Arsenic induces hepatic insulin resistance via mtROS-NLRP3 inflammasome pathway. *J Hazard Mater*. 2020;399:123034. doi:10.1016/j.jhazmat.2020.123034.
  56. Sousa AR, Lane SJ, Nakhosteen JA, Lee TH, Poston RN. Expression of interleukin-1 beta (IL-1 $\beta$ ) and interleukin-1 receptor antagonist (IL-1ra) on asthmatic bronchial epithelium. *Am J Respir Crit Care Med*. 1996;154(4 Pt 1):1061–1066. doi:10.1164/ajrccm.154.4.8887608.
  57. Thawanaphong S, Nair A, Volfson E, Nair P, Mukherjee M. IL-18 biology in severe asthma. *Front Med (Lausanne)*. 2024;11:1486780. doi:10.3389/fmed.2024.1486780.
  58. Xu ZP, Huo JM, Sang YL, Kang J, Li X. Effects of arsenic trioxide (As<sub>2</sub>O<sub>3</sub>) on airway remodeling in a murine model of bronchial asthma. *Can J Physiol Pharmacol*. 2012;90(11):1576–1584. doi:10.1139/y2012-127.
  59. Milde-Langosch K, Röder H, Andritzky B, Aslan B, Hemminger G, Brinkmann A. The role of the AP-1 transcription factors c-Fos, FosB, Fra-1 and Fra-2 in the invasion process of mammary carcinomas. *Breast Cancer Res Treat*. 2004;86(2):139–152. doi:10.1023/b:Brea.0000032982.49024.71.

To cite this article: Single SL, Hough KP, Sivan S, Athar M, Goliwas KF, Deshane JS. Heavy Metal Exposure Alters Immunological Pathways Involved in Asthma Pathogenesis. *European Journal of Respiratory Medicine*. 2025; 7(1): 468- 482. doi: 10.31488/EJRM.154.

© The Author(s) 2025. This is an open access article distributed under the terms of the Creative Commons Attribution License (<https://creativecommons.org/licenses/by/4.0/>).